Structural Characterization and Electron Tunneling at *n*-Si/SiO_2/SAM/Liquid Interface

Y. Gu, B. Akhremitchev, G. C. Walker, and D. H. Waldeck*

Chemistry Department, University of Pittsburgh, Pittsburgh, Pennsylvania 15260

Received: September 22, 1998; In Final Form: May 1, 1999

Alkylsilane-based self-assembled monolayer films were prepared on *n*-Si with a thin oxide (nominally SiO_2) layer. The surface morphology was characterized by atomic force microscopy (AFM). Photocurrents between the *n*-Si and a redox species in liquid solution were also examined as a function of the alkane chain length of the self-assembled monolayer (SAM) molecules. They demonstrate that the films are compact and that current flow is blocked by the alkane monolayer, displaying a significant decrease with increasing chain length of the alkane.

Introduction

This study describes the investigation of electron transfer in chemically modified silicon electrodes. Such studies are important from both fundamental and practical perspectives. Electron transfer is a fundamental process which is ubiquitous in chemical and biological transformations. Although the understanding of intramolecular and intermolecular electron transfer has evolved dramatically over the past few decades, an understanding of heterogeneous electron transfer has lagged behind. Recently, however, considerable progress is being made in this area, and it has largely been driven by the discovery of methods for chemically controlling and/or stabilizing the properties of solid electrode interfaces.[1−6] Electron transfer and chemistry of Si/SiO_2 structures is also important to device fabrication, because the SiO_2-covered *n*-Si surface plays a key role throughout the integrated circuit fabrication process. The monolayer formed on the SiO_2 surface could potentially be used as an etching mask,[7] an adhesion promoter, or an extra barrier for suppressing gate leakage current.[8]

The study reported here investigated electron transfer between a silicon electrode in which an insulating barrier was purposely placed on the surface of the electrode and ferrocyanide in solution. This barrier was created by first growing a thin (10−20 Å) oxide film on the silicon substrate and then coating this oxide film with an alkylsiloxane self-assembled monolayer (SAM) film. By systematically changing the chain length of the alkyl group, one can control the thickness of the organic layer. These monolayer films have been studied using a wide variety of methods.[9] Typically, the films form compact, hydrophobic layers which are highly ordered and resistant to the transport of water and aqueous ions.[10] Most of the earlier work characterizing the formation mechanism has focused on monitoring the kinetics of the formation process.[11,12] The structural studies here provide evidence for the formation of domains, or 'islands', on the oxide layer at intermediate coverages. This observation suggests a growth mechanism in which monolayer islands initially form at nucleation sites and then grow in size until they coalesce into a uniform film.[9,13,14]

A number of workers have explored the electrical characteristics of chemically modified silicon surfaces. The siloxane chemistry has been exploited to create modified electrodes for photoelectrochemical systems, either structures with insulating barriers[15] or with redox active moieties tethered to the electrode.[16] Workers[8] have also used this chemistry to make metal−insulator−semiconductor (MIS) diodes which have 'ultrathin' insulating barriers. More recently, other chemical approaches to the alkylation of *n*-Si surfaces have begun to be developed. These include halogenation/alkylation methods as well as radical-based olefin addition routes.[3,4] Such structures are desirable because they contain a single barrier layer on the silicon rather than the intermediate SiO_2 layer that is required in the presently used approach. The monolayers prepared by these methods on Si surfaces, although they appear to stabilize the surface,[4b] are not yet compact or complete enough to block electrical current to a reasonable extent.

The photocurrent studies reported here aim to investigate how the electron transfer depends on the thickness of the self-assembled alkylsiloxane film. Previous work in this area has investigated the electron tunneling at Au/SAM/electrolyte interfaces,[2] *n*-InP/SAM/electrolyte interfaces,[6,17] and in Al/Al_2O_3/SAM/Al sandwich structures at 77 K.[18] The distance dependence (or thickness dependence) of the electron transfer in these systems was found to be consistent with the distance dependencies found for electron transfer rates in intramolecular systems. In contrast, the thickness dependence of the electron transfer in the silicon system (reported here) is found to be shallower, or weaker. On the other hand, the thickness dependence reported here for the silicon system is found to be steeper, or stronger, than that recently reported for *n*-Si/SiO_2/SAM/Al diodes.[8] Possible explanations for this behavior are discussed.

Experimental Methods

Preparation of an Alkylsilane Monolayer on a Si/SiO_2 Surface. The *n*-Si wafer was purchased from Virginia Semiconductor, Inc. The resistivity of the sample was reported to be $\leq 0.005\ \Omega$ cm which corresponds to 10^{19} cm^{-3} or larger donor density.[19,20] The wafer was sliced into rectangular pieces with the approximate dimensions 3 cm × 0.5 cm. The samples were degreased by boiling in ethyl alcohol for 10 min and were then etched with 10% HF for 5 min to remove the native oxide. A SiO_2 overlayer was grown on the freshly etched surface by placing the sample in a solution of concentrated H_2SO_4 and 30% H_2O_2 (70:30 v/v)[21,22] (*Please note that "piranha" solution reacts violently with many organic materials and must be treated with great care*). This mixture was heated to 90 °C and held there for 25 min, then it was cooled to room temperature and the liquid was pulled off. The silicon slice was immediately rinsed with water and blown dry by high purity N_2. This surface is completely wetted by water.

The cleaned Si strips were placed in a vial that was previously cleaned by boiling in ethyl alcohol for 20 min and oven drying

10.1021/jp9838184 CCC: $18.00
Published on Web 06/03/1999

at 120 °C. This vial contained approximately 20 mL of a 0.5% (by weight) solution of alkyltrichlorosilane (United Chemical Technologies) in bicyclohexyl (Fluka). Also, 10−20 drops of CCl_4 was added to the solution from a micropipet. The CCl_4 is believed to promote the formation of the monolayer. The container was sealed from the air, and monolayer formation was allowed to proceed for approximately 1 h. The sample was removed from the vial and thoroughly rinsed with $CHCl_3$ and then ethanol to remove any residual organic contaminants. The substrate was then dried with a mild flow of N_2 gas. Contact angle measurements on these surfaces revealed very hydrophobic surfaces that formed contact angles of 115(±1)° with water for all the alkyl chain lengths.

The samples were then sliced into 0.5 cm × 0.5 cm squares for electrode preparation. To study the photocurrent versus chain length, the 0.5 cm × 0.5 cm pieces of a single oxidized silicon wafer were immersed in solutions containing different alkylsilanes. This procedure was used to ensure that the oxide thickness was the same for the different alkyl chain lengths. The area of the electrodes was determined by measurements with a caliper.

Electrodes and Photocurrent Experiment. The method used to prepare the electrode for the experiment has been described previously.[15] Briefly, the film from one side of the Si crystal was rubbed off. A eutectic mixture of In and Ga was rubbed onto the exposed (backside) Si surface. A copper pin was attached to the eutectic mixture, and the assembly was glued together with epoxy.

The details of the photocurrent experiment have also been described previously.[6,17] The solution used for the photocurrent experiment was 0.080 M $K_3[Fe(CN)_6]$/0.080 M $K_4[Fe(CN)_6]$ in a 0.50 M aqueous solution of K_2SO_4. The light source used for the photocurrent experiment was a semiconductor diode laser operating at a wavelength of 650 nm. The intensity used in this study was 0.3 mW/cm^2 unless reported otherwise. The bias voltage between the electrode and the solution was held constant at 0.0 V versus SCE (saturated calomel electrode) during the experiment. The laser beam was chopped by a mechanical chopper and the photocurrent signal was detected using a Stanford Research Systems (model SR530) lock-in amplifier.

The apparatus used to measure the capacitance−voltage profiles has been described previously.[23] It is a lock-in (model SR530) based method which allows the measurement to be performed at frequencies from 100 Hz to 10 kHz. Measurements were performed over this range but those given in the paper were measured at 1 kHz. No significant frequency dependence for the Mott−Schottky plots was found over this range.

Surface Morphology—Atomic Force Microscopy (AFM). The AFM experiment was performed with a Digital Instruments Multimode (Santa Barbara, CA) scanning force microscope, operating in contact mode in air. An oxide-sharpened silicon nitride probe was used in the experiment (Digital Instruments). The tip radius of curvature can range from 5 to 40 nm (manufacturer's specification). The apparent lateral size of 2 nm high surface features increases by 8 nm to 25 nm for the specified radius range because of tip shape convolution effects. For objects with a lateral size of 250 nm, this effect can result in a 6−20% overestimate of the surface coverage.

The Si sample used for the AFM experiment was coated with an octadecyltrichlorosilane monolayer on half of its surface. Figure 1 shows the configuration used to prepare the sample so that only half of it was coated. This sample was classified into four different regions. Region A of the sample was not directly exposed to the octadecyltrichlorosilane and is not coated with the monolayer. Region B is very close to the part of the sample that is immersed in the fluid and has a partial coating of the monolayer. Region C is dipped in the solution but is very close to the uncoated region. It is more densely coated than region B, but the film is by no means compact. Region D is the part of the wafer that is completely immersed in the solution and shows a compact monolayer film.

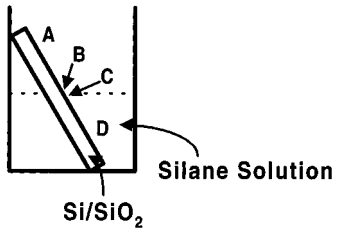

Figure 1. Illustration of the method used to prepare a partially coated alkylsiloxane film for investigation using atomic force microscopy (AFM). The four areas imaged by the AFM are designated as A, B, C, and D.

Characterization of the Si/SiO_2/Alkane Monolayer Films

The films formed on thin oxide coatings on silicon with the method described above have been prepared for some time and characterized in a number of ways by other workers.[9] A few AFM studies of these systems have been reported.[7,13,14]

Surface Morphology of Octadecylsiloxane Monolayers. Atomic force microscopy (AFM) was used to investigate the thickness of the monolayer films formed on the SiO_2 and to characterize the film morphology. By deliberately creating an electrode which was fully coated on one end but only partially coated or not coated on the other end, it was possible to infer important information concerning the nature of the monolayer formation and to characterize the compactness of the film.

AFM images of the different regions A, B, C, and D were performed (see Figure S1 of the Supporting Information). The results of these data show that the monolayer growth occurs by island formation and then coalescence into a compact film, as reported earlier for related systems.[13,14] The formation of the island structure suggests a mechanism for the monolayer formation in which an alkylsilane molecule first adsorbs on the surface but is mobile enough that it can find a more stable site where nucleation has already occurred. It seems likely that the alkylsilane diffuses along the surface until it is trapped near an island, but it may be that the adsorbate desorbs and adsorbs again until it finds a stable site on the surface. The irregularity in the island boundaries (see Figure 2, top image) suggests the existence of strong binding between the alkylsiloxane molecule and the substrate once it reaches a site on the surface which is near an island. Nevertheless, it is evident that when molecules assemble together the chemical bond between the substrate and the molecule is formed quickly enough and is strong enough to prevent significant annealing of the island perimeter. These observations are consistent with other studies which investigated the morphology of these films and defects designed into them.[8,13,14,22]

In the partially coated region, it is also possible to analyze the height of the islands. Figure 2 shows an image for which the height of the "island" structures was measured. It is evident from the scale bar that the thickness is about 2 nm. A more quantitative analysis of this image gives an average film height of 1.8 ± 0.2 nm, indicating the formation of monolayer thick structures. This value is slightly less than the chain length expected for an octadecylsilane molecule (ca. 2.3 nm). Komeda et al.[7b] prepared a partially covered sample by dipping in an OTS solution for a short amount of time, and they observed

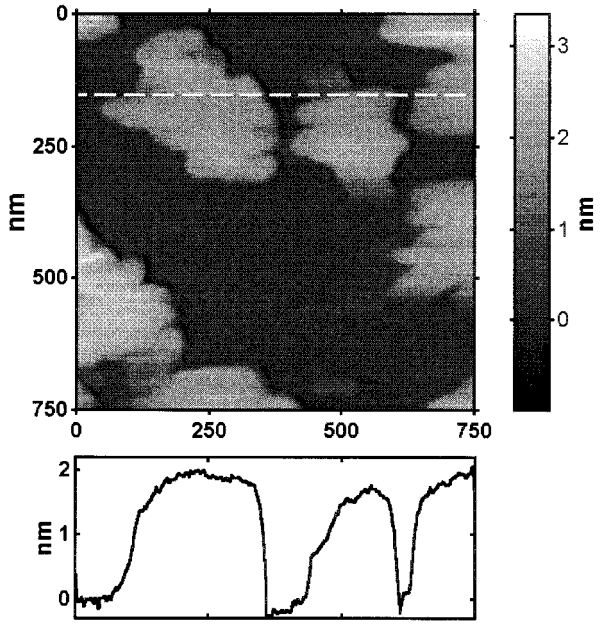

Figure 2. A 750 nm × 750 nm AFM topography image of a partially coated sample.

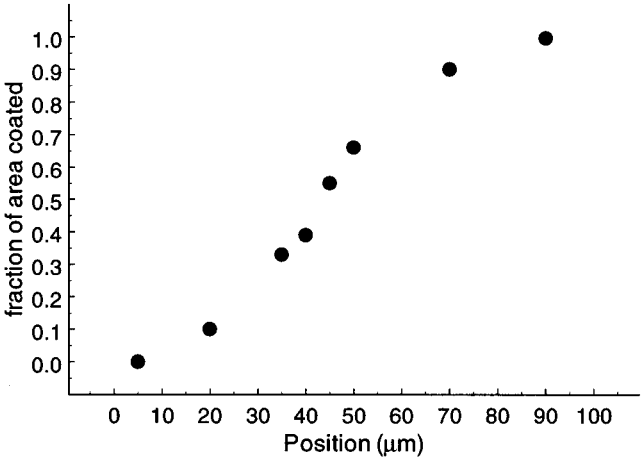

Figure 3. Plot of the alkylsiloxane coverage versus the position along the substrate.

island formation. They found an island height that was approximately 1.5 nm and interpreted this as resulting from the limited time for growth that was allowed by their preparation procedure. One possible explanation for this observation is that the tip compresses the monolayer somewhat when it scans across the surface. Alternatively, the chains could be tilted from the surface normal in the islands, rather than being oriented perpendicular to the surface of the substrate, as has been found for the case of complete films.[9]

Important characteristics of the film for electrical measurements are its compactness and coverage, which will influence its ability to act as an insulating barrier to current. Figure 3 shows a plot of the alkylsiloxane coverage as a function of the distance along the substrate. The coverage was obtained by integrating the area of the structures (≥1.5 nm) in an image and comparing it to the total area of the image. In region A, where the surface was not exposed to the alkylsilane, there is no coverage. In the intermediate zone (regions B and C), the coverage changes dramatically. In region D, the coverage is uniform with a value of 99.5% or higher. A limitation to this analysis is that the spatial resolution available to the AFM here is approximately 20 nm, so defects and structures smaller than this size are not readily evident. In region D, the images were integrated over wide regions (hundreds of micrometers) and found to be uniform. If large patches do exist in the film structure, they would need to be larger than this size range and would be evident to the eye or under an optical microscope.

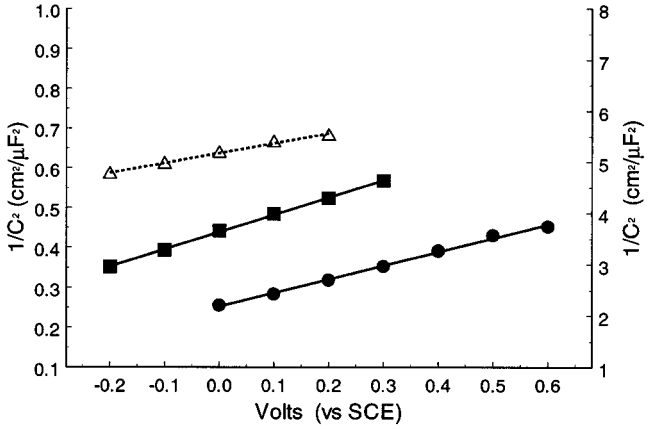

Figure 4. Capacitance−voltage characteristics for three different electrode structures: (●) etched silicon electrode; (■) SiO_2-coated silicon electrode; (△) SAM/SiO_2-coated silicon electrode. The open symbols correspond to the right *y*-axis scale, and the filled symbols correspond to the left *y*-axis scale. In each case, the data is well fit by the Mott−Schottky relation (as indicated by the best fit lines plotted with the data).

Characterization of the Oxide Film Thickness. A number of methods may be used to characterize the thickness of the oxide overlayer on a *n*-Si substrate, including ellipsometry, capacitance measurements, and X-ray photoelectron spectroscopy (XPS). The characterization reported here includes XPS and capacitance studies on oxide films that were prepared on *n*-Si substrates.

The energy shift in the 2p core level of Si was used to determine the presence of the oxide film on the silicon substrate. The XPS spectra reveal a peak for the *n*-Si substrate at 98.4 eV binding energy, which is consistent with that for elemental silicon, and a second peak at 102.6 eV binding energy, which is consistent with that of Si in an SiO_2 environment.[24] A comparison of the relative intensities of the two peaks may be used to determine the thickness of the oxide film. To obtain a thickness for the film, the escape depth of the photoelectrons from the surface was taken to be 2.45 nm.[25] Using this value and the relative peak areas, the oxide thickness is found to be 1.2 nm.

Capacitance−voltage profiles of the Si substrate and the coated electrodes were also collected. The silicon substrate was cleaned and etched with HF in the manner described above. Then it was immersed in a 0.10 M Na_2SO_4 aqueous solution. A Mott−Schottky analysis of the data[27] revealed a linear region of only about 0.5−0.6 V in size (see Figure 4). The dopant density obtained from these data is $4-5 \times 10^{19}$ cm^{-3}, which is in reasonable agreement with the manufacturer's quotation. The flat band potential, found by extrapolation of the line, is −0.74 ± 0.05 V versus SCE. The limited range of linearity probably has several sources. The high dopant density of the material makes the space charge capacitance higher than in a lower doped material, and hence the measured capacitance will be more susceptible to capacitances in series with the space charge layer, caused by oxide growth on the surface and corrosion of the surface during the measurement.[26,27]

Figure 4 also shows the capacitance voltage profile for an oxide-coated *n*-Si electrode. The upward shift of the capacitance voltage curve is consistent with the high dopant density of the

Si and the presence of the insulating overlayer. Using the depletion approximation and taking the silicon dopant density to be 4×10^{19} cm^{-3}, one expects a depletion layer width of only 4.0 nm and a capacitance of 2.7 μF/cm^2, with a potential drop of 0.5 V across the space charge layer. An SiO_2 film (take $\epsilon_{SiO_2} = 3.6$) of thickness 1.2 nm has a capacitance of 2.6 μF/cm^2, using a parallel plate model. Hence, the capacitance of the 'effective', voltage-dependent capacitor in the semiconductor (i.e., the space charge region) is similar in magnitude to the capacitance of the oxide layer in series with it. The total capacitance of the electrode is the serial capacitance of the bulk material and the oxide overlayer. The upward shift of the capacitance-voltage characteristic shown here gives a thickness for the SiO_2 layer of 1.4 nm when the dielectric constant of the SiO_2 is taken to be 3.6. This value is in good agreement with the 1.2 nm width found independently using the XPS method. Because of the limited range of voltage, the curvature in the Mott−Shottky plot is not evident. The further decrease in the capacitance when the SAM overlayer is grafted onto the oxide occurs for reasons similar to that described for the oxide layer.[28] The reduction in the slope of the plot can be explained by an additional voltage drop across the SAM overlayer.

Photocurrent/Tunneling Experiments

A measurement of the photocurrent generated by electron transfer between the coated silicon electrodes and a redox species in solution can be used to investigate how the electron-transfer rate constant depends on the thickness of the insulating film. The measured photocurrent may be expressed as

$$j_{\text{photo}} = k_{\text{ET}}[h_s][D] \tag{1}$$

where k_{ET} is the rate constant, h_s is the surface hole concentration, and D is the donor ($Fe(CN)_6^{4-}$) concentration in the solution. By quantifying the concentrations of the donor and the holes, one can obtain the electron transfer rate constant and examine its dependence on properties of the film. In the studies described below, the donor concentration in solution and the surface hole concentration are held constant while the photocurrent is examined as a function of the alkane chain length of the alkylsilane monolayer film. To the extent that the donor concentration and the hole concentration remain fixed, this measurement examines the dependence of the electron-transfer rate constant on the thickness of the insulating film. For the situation where the insulating film forms a tunneling barrier, one expects the rate constant to decrease exponentially as the thickness of the barrier increases, i.e., $\exp(-\beta r)$, where β is the tunneling parameter and r is the thickness.

The photocurrent is measured on Si/SiO_2 electrodes that are coated with different alkylsilanes whose alkane chain lengths vary. The redox couple is an equimolar mixture of ferricyanide and ferrocyanide at 0.080 M. The bias potential applied to the electrode was 0 V versus SCE. The $j-V$ curves for systems of this sort have been reported previously.[15] The intensity of the light was varied from 0.050 to 0.50 mW/cm^2. In Figure 5, the natural logarithm of photocurrent magnitude is plotted as a function of the number of methylene units in the alkane chain for two different light intensities. The error bars represent an average of measurements on three different electrodes. The tunneling constant β that is obtained from the slope of these lines is -0.29 ± 0.1 at 0.30 mW/cm^2 and -0.23 ± 0.09 at 0.050 mW/cm^2. The tunneling constant observed with these systems is significantly smaller than that which has been reported for alkanethiol monolayers on gold electrodes[2] and on *n*-InP.[6,17] However, it is significantly steeper than that reported by others for silicon-based systems.[8]

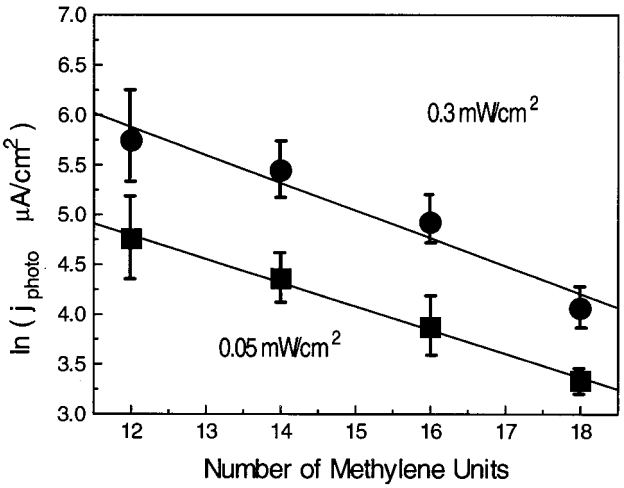

Figure 5. Plot of ln j_{photo} versus the number of methylene units in the monolayer film is shown for two different light intensities. The lines represent a best fit to the experimental data. The slopes of the two lines are -0.23 for 0.05 mW/cm^2 and -0.29 for 0.3 mW/cm^2.

As described above, the photocurrent's thickness dependence will represent solely a dependence on the electron transfer rate only if the concentrations of the redox couple and the hole concentration are not changing. The redox couple is present in solution at high excess concentration so that the photocurrent is not mass transport limited. Other studies[15,26] show that this redox concentration is able to support much higher current densities than those observed here. Control of the surface hole concentration is more difficult to demonstrate however. This difficulty arises from the interplay between the nonradiative relaxation processes (including hole transfer to the electrolyte) and the injection level of photocarriers in the material. The highly doped *n*-Si used here was chosen because its fast nonradiative recombination rate fixes the surface hole concentration even though the hole transfer rate to the solution is changing.

A number of workers[29−33] have provided analytical treatments of the photocurrent−voltage characteristics of illuminated semiconductor/electrolyte systems and how these characteristics are affected by the recombination pathways in the semiconductor material. Although these treatments do not include an insulating barrier, they are useful as a quantitative guide to assess how the surface hole concentration changes. The model used here includes the effects of surface recombination and space charge recombination in an explicit manner.[30] McCann and Haneman[30] solved the continuity equation for photogenerated holes in the steady-state limit and obtained the following expression for the hole current at the interface $J_p(0)$:

$$J_p(0) = i_p(0)\left[\frac{i_p(0) + qI_0\left(1 - \frac{\exp(-\alpha w)}{1+\alpha L_p}\right) + J_0 - \int_0^w q\frac{p(x) - p^0(x)}{\tau_p(x)}dx}{i_p(0) + J_0 \exp\left(\frac{qV_{h\nu}}{kT}\right)\exp\left(\frac{E_{fp}(0) - E_{fp}(w)}{kT}\right)} - 1\right] \tag{2}$$

where α is the absorption coefficient, L_p is the hole diffusion length, J_0 is the reverse saturation current, q is the electronic charge, I_0 is the absorbed light flux, $p(x)$ is the hole concentration at x under illumination, $p^0(x)$ is the hole concentration in the

dark, $\tau_p(x)$ is the decay rate of holes at position x, w is the depletion layer width, and $V_{h\nu}$ is the photovoltage. The exchange current $i_p(0)$ is given by the product $qv_{et}p^0(0)$, where v_{et} is the hole transfer velocity and $p^0(0)$ is the surface concentration of holes in the dark. The integral in the numerator of eq 2 contains the surface and space charge recombination processes. McCann and Haneman evaluate the integral for the recombination parameters in an approximate manner and find the spatial dependence of the quasi-Fermi levels $E_{fp}(x)$ through an appropriate choice of boundary conditions (see ref 30 for details). It is possible to find the surface concentration of holes, $p(0)$, via the fundamental relation

$$J_p(0) = i_p(0)\left[\frac{p(0)}{p^0(0)} - 1\right] \tag{3}$$

By neglecting the recombination in the space charge region (which is very narrow for the highly doped Si), the recombination integral may be evaluated to give the surface recombination current as $qv_{SR}\Delta p(0)$, where $\Delta p(0)$ represents the concentration of photogenerated holes. With these approximations it is possible to evaluate the integral and find an analytical expression for the recombination current (and also surface hole concentration) in terms of the model parameters and *n*-Si parameters.

Figure 6A shows photocurrent−voltage curves that were calculated by this model using parameters that are appropriate for *n*-Si.[34] In these simulated profiles, the open circuit potential is the value of the potential where the photocurrent is zero. The two dotted curves (i.e., dotted and dot−dashed) show simulations for a silicon electrode whose properties are similar to that reported by Lewis.[35] For the case where no surface recombination occurs (dotted curve), the open circuit photovoltage is 0.62 V, and with a surface recombination velocity of 10^3 cm/s (dot−dashed curve), it is found to be 0.59 V. This result is in reasonable agreement with the values reported in ref 35. The dashed and solid curves show simulations for the highly doped silicon whose parameters are given in ref 34. The different curves shown are for different hole transfer rates and surface recombination velocities. It is clear from these curves that the open circuit photovoltage will not exceed 0.4 V for the highly doped samples. The open circuit photopotential of an uncoated *n*-Si electrode in contact with the ferricyanide/ferrocyanide solution was measured to be 25 ± 25 mV. This value of the photovoltage is consistent with a surface recombination velocity in excess of 10^4 cm/s and a low charge injection velocity (less than 0.5 cm/s). Of course, the silicon surface is not stable under these conditions, and this comparison is made only to indicate that the recombination and/or corrosion on this surface is rapid.

Figure 6B shows the surface hole concentrations that are calculated for the highly doped silicon with this same model. The different surface recombination and hole transfer rates are given in the figure caption. The dotted and solid curves in this figure correspond to the case of a zero surface recombination velocity. In this case, the change in the electron-transfer rate has a dramatic effect (10^2−10^3) on the concentration of photogenerated holes at the surface. The dashed curves show simulations for the more realistic situation in which surface recombination is included. Even moderate surface recombination velocities can be used to control the concentration of surface holes. For the simulations shown here, the surface recombination velocity is taken to be 1000 cm/s. This value, and higher ones, are sufficient to keep the surface hole concentration fixed to within 1% when the charge-transfer rate changes by a factor of 100. This simulation supports the assumption that the surface

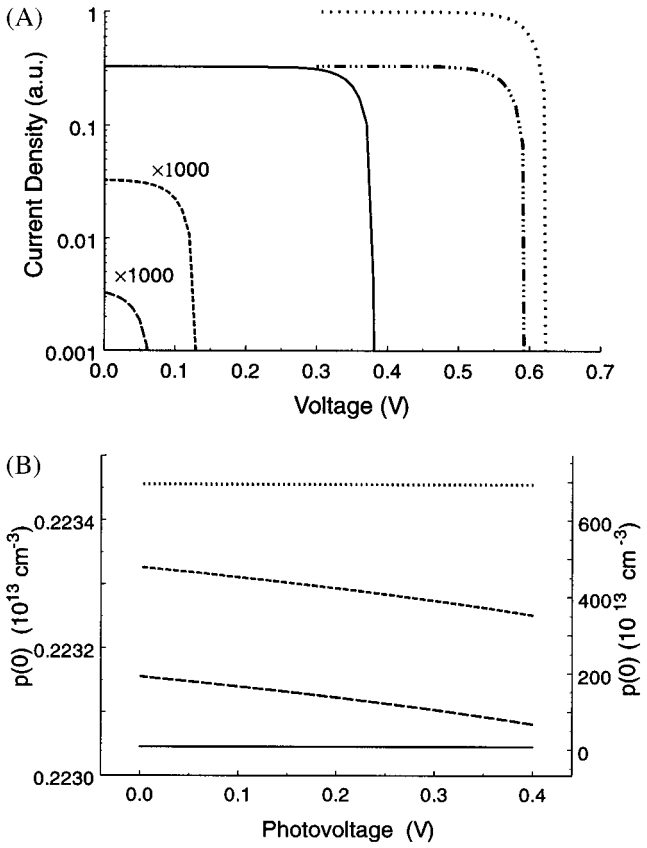

Figure 6. (panel A) Simulated photocurrent−voltage curves for a Si electrode. The dotted curves correspond to a silicon electrode with a dopant density of 10^{17} cm^{-3}. The surface recombination velocity is 0 cm/s for the dotted curve and 10^3 cm/s for the dot−dashed curve The solid curve and the dashed curves are for the high dopant density Si (10^{19} cm^{-3}). The surface recombination velocity is 0 cm/s for the solid curve, 5×10^4 cm/s for the dashed curves. The charge-transfer velocity is 0.5 cm/s for the long dashed curve and 5 cm/s for the other curves. (panel B) Surface hole concentrations that are found from the simulations. The solid curve and dotted curve (scaled to the right *y*-axis) correspond to a zero surface recombination velocity and charge-transfer velocities of 5 cm/s (dotted line) and 0.05 cm/s (solid line). The dashed curves (scaled to the left *y*-axis) correspond to a surface recombination velocity of 1000 cm/s and charge-transfer velocities of 5 cm/s (short dashed line) and 0.05 cm/s (long dashed line).

hole concentration in the series of electrodes studied here is not changing.

The simulations shown here are meant as a guide and an estimate for the order of magnitude of the surface recombination rate. A number of limitations in the model, when compared with the present system, have an impact on the quantitative reliability of the recombination velocities and hole concentrations. One significant issue is that the model uses a Maxwell−Boltzman expression to treat the carrier concentrations. Although appropriate for nondegenerate semiconductor materials, that approach is not correct for a degenerate semiconductor like the one studied here. This limitation can cause errors of up to 20% in the carrier densities, for the dopant level used in this study.[36] Second, although the model incorporates recombination in the space charge region, that effect was not used in the simulations. The depletion layer is quite thin for this highly doped material, and this effect is not expected to be significant. A third issue relates to the treatment of surface recombination by the model. The model does not allow this quantity to be dependent on the voltage nor does it incorporate any kinetics for the trapping and recombination via surface states. These effects have been

reported in other systems,[37] but their generality is not yet clear. For these reasons, the values of the hole concentrations found from the simulations are not used in the data interpretation. The value of the surface recombination velocity found from the simulations in Figure 6A is taken to be reliable to an order of magnitude and to represent a lower bound on its true value. The major conclusion that is drawn from these simulations is that the hole concentration at the surface is controlled by the internal nonradiative recombination in the semiconductor and not by hole transfer to the electrolyte.

The operation of this device under illumination is a very complex system; many factors, such as Fermi level shifts and recombination rates, have to be known or quantified in order to accurately determine the surface hole concentration and extract a rate constant. However, one expects the concentration of holes to rise as the light intensity increases and as the hole transfer rate through the film decreases. Figure 5 shows a significant increase in the photocurrent with light intensity, which is consistent with higher hole concentrations at the surface. In addition, the data reveal little or no change of the tunneling parameter β on the light intensity. These observations are consistent with a model in which nonradiative relaxation pathways, other than photocurrent generation, control the surface concentration of holes. This behavior was also observed in a previous study on *n*-InP/thioalkane systems.[17]

Discussion and Conclusions

The electrical transport and surface morphology of *n*-Si−SiO_2−alkylsiloxane monolayer structures were investigated. The investigations used highly doped (10^{19} cm^{-3}) *n*-Si upon which a thin (10−20 Å) oxide film was chemically grown. On top of the oxide, a monolayer film of alkylsiloxane was prepared. The monolayer films were characterized using AFM imaging and by capacitance−voltage measurements. The ability of the films to block current was investigated by using photocurrent measurements in a photoelectrochemical cell.

The AFM studies were used to characterize the film thickness and the film's "compactness". The thickness measured for the C18 chains was observed to be compatible with the alkane chain oriented more or less perpendicular to the surface of the electrode. The films were observed to have a very high coverage (>99.5%). At intermediate coverages, it was found that the film grew by the formation of islands. The size and shape of these domains is consistent with a strong interaction between the alkylsilane and the surface, rather than a system in which the alkylsilane is highly mobile and can anneal. As the film coverage increases, these domains appear to increase in size and coalesce. Although domain walls are clearly evident at intermediate coverages, they become less evident at higher coverages. In part, this may be caused by the limited lateral spatial resolution of the AFM. For high coverage surfaces, there do not appear to be defects in the film whose lateral size is about 4 nm or larger. The method used to prepare the sample for AFM studies presented here is unique. The information obtained from these surface morphology studies agrees with earlier studies of the formation mechanism of the SAM. The relatively defect-free film images indicate that the system is useful for tunneling experiments.

The photocurrent between the device and a redox couple in the electrolyte solution was measured as a function of the alkane chain length. The tunneling constants obtained in this series of experiments ranged from 0.2 to 0.3 per methylene. This value is considerably higher than that found by others for insulating barriers on silicon structures. The work[8] on *n*-Si−SiO_2−alkane−Al structures (a metal−insulator−semiconductor (MIS) device) showed no dependence of the tunneling current on the length of the alkane chain, despite a very large decrease in the sample conductivity that could be associated with the presence of the alkane. This result is certainly surprising in light of the large amount of literature which indicates a strong dependence of tunneling on the chain length. More recently, Lewis[4] has reported current−voltage curves on alkylated silicon electrodes, which indicates little or no attenuation of the current by the chemical monolayer film. In this latter case, the origin of this insensitivity may be related to the open structure of the film. An attempt was also made to prepare films using the method reported by Chidsey.[3] Although layers were obtained with contact angles for water of 110°, their ability to block current flow was also poor. This observation agrees with the open structure of these films, as reported by Chidsey.[3]

In addition, the tunneling parameter observed here is significantly weaker than that found in other electrochemical systems. For example, on gold electrodes coated with alkylthiols and hydroxy-terminated alkylthiols, the tunneling constants are observed to be between 0.9 and 1.1 per methylene unit.[2] On *n*-InP, such studies give tunneling constants which range between 0.4 and 0.6 per methylene unit.[6,15] Early studies on tunneling in Al/Al_2O_3/SAM/Al structures observed no dependence on alkyl chain length at room temperature, but it was found to decay as ~1.2 per methylene at 77K.[18] The origin of the differences in thickness dependence for the different systems is still not clear. Two possible explanations for the tunneling parameter reported here are discussed below.

Some of the variability in these tunneling parameters may result from differences in the number and size of defects in the films, i.e., pinholes and defects where the conductivity is higher than it is through the alkane layer. If the number of pinholes became larger as the length of the alkane chain increased, then one would observe a tunneling parameter that is smaller than the actual value. Although no direct evidence exists to refute this explanation, the high contact angles which the layer makes with water for all of the different length films and the few defects observed in the AFM images of the C18 films indicate that this explanation is not likely. By assuming a flat surface, one can analyze the contact angles formed with water to estimate the fractional area of the surface that is not coated.[38] For this system, one finds that it is less than 1%, which is consistent with the AFM data. Yet these data are only circumstantial, it will be necessary to perform the tunneling experiments using a proximal probe method to address this mechanism conclusively.

The Si system studied here differs from the Au and InP systems by having a double insulating barrier, the SiO_2 and the alkane chain. If two different current mechanisms are operating in series, i.e., electron current through defect sites in the oxide layer followed by tunneling through the monolayer, and have similar rates, then one could observe a shallow distance dependence. If the transport through the oxide operates with the rate k_{ox} and that through the alkane film with a rate k_{alk}, then the total rate k_{total} will be given by

$$k_{total} = k_{alk}\left[\frac{1}{1 + k_{alk}/k_{ox}}\right]$$

When the transport through the oxide film is much faster than that through the alkane, then one will observe a total rate that is the same as k_{alk} and the thickness dependence will reflect the distance dependence of k_{alk} (which is expected to be exponential, i.e., tunneling). In contrast, if the rate of k_{ox} is much smaller than k_{alk}, then the total rate will behave as k_{ox}. Depending on

the preparation and nature of the oxide film, k_{ox} could have an exponential distance dependence (oxide acts as a tunneling barrier) or have a very weak distance dependence (e.g., a hopping conductivity through traps in the film). When the two rates are similar, then the distance dependence would be intermediate. A more detailed study in which the different rates can be disentangled or where the dynamic range is large enough to observe the transition from one regime to the other is required to address this hypothesis.

This report describes photocurrent experiments through tunneling barriers formed on *n*-Si/SiO_2/SAM structures in electrolyte solutions. The observed dependence of the photocurrent on the chain length of the alkane units in the SAM was found to be steeper than that reported for an MIS diode prepared in a similar manner,[8] but is shallower than that reported for other systems.[2,6,15,18] Two possible mechanisms for the distance dependence were discussed.

Acknowledgment. This work was supported by the Department of Energy, Division of Chemical Sciences (DE-FG02-89ER14062), and the Office of Naval Research (ONR N0001-96-1-0735). We acknowledge useful discussions with R. Naaman. We thank S. Trakhtenberg for showing us how to prepare the alkylsiloxane films. D.H.W. acknowledges a Belkin Visiting Professorship at the Weizmann Institute of Science during part of this work. B.A. acknowledges a Mellon Graduate Fellowship.

References and Notes

(1) Lewis, N. S. *J. Phys. Chem B* **1998**, *102*, 4843.

(2) (a) Cheng, J.; Saghi-Szabo, G.; Tossell, A. J.; Miller, C. J. *J. Am. Chem. Soc.* **1996**, *118*, 680. (b) Chidsey, C. E. D. *Science* **1991**, *251*, 919. (c) Smalley, J. F.; Feldberg, S. W.; Chidsey, C. E. D.; Linford, M. R.; Newton, M. D.; Liu, Y.-P. *J. Phys. Chem.*, **1995**, *99*, 13141. (d) Finklea, H. O.; Hanshew, D. D. *J. Am. Chem. Soc.* **1992**, *114*, 3173.

(3) (a) Linford, M. R.; Chidsey, C. E. D. *J. Am. Chem. Soc*. **1993**, *115*, 12631. (b) Linford, M. R.; Fenter, R.; Eisenberger, P. M.; Chidsey, C. E. D. *J. Am. Chem. Soc*. **1995**, *117*, 3145. (c) Terry, J.; Linford, M. R.; Wigren, C.; Cao, R.; Pianetta, P.; Chidsey, C. E. D. *Appl. Phys. Lett*. **1997**, *71*, 1056.

(4) (a) Bansal, A.; Li, X., Lauermann, I.; Lewis. N. S.; Yi, S. I.; Weinberg, W. H. *J. Am. Chem. Soc*. **1996,** *118*, 7225. (b) Bansal, A.; Lewis, N. S**.** *J. Phys. Chem. B* **1998**, *102*, 1067.

(5) (a) Gu, Y.; Lin, Z.; Butera, R. A.; Smentkowski, V. S.; Waldeck, D. H. *Langmuir* **1995**, *11*, 1849. (b) Gu, Y.; Kumar, K.; Lin, Z.; Read, I.; Zimmt, M. B.; Waldeck, D. H. *J. Photochem. Photobiol. A* **1997**, *105*, 189.

(6) Gu, Y.; Waldeck, D. H. *J. Phys. Chem.* **1996**, *100*, 9573.

(7) (a) Lercel, M. J.; Tiberio, R. C.; Chapman, P. F.; Craighead, H. G.; Sheen, C. W.; Parikh, A. N.; Allara, D. L. *J. Vac. Sci. Technol. B* **1993**, *11*, 2823. (b) Komeda, T.; Namba, K.; Nishioka, Y. *Appl. Phys. Lett*. **1997**, *70*, 3398. (c) Komeda, T.; Namba, K.; Nishioka, Y. *Jpn. J. Appl. Phys*. **1998**, *37*, L204.

(8) (a) Boulas, C.; Davidovits, J. V.; Rondelez, F.; Vuillaume, D. *Phys. Rev. Lett*. **1996**, *76*, 4797. (b) Vuillaume, D.; Boulas, C.; Collet, J.; Davidovits, J. V.; Rondelez, F. *Appl. Phys. Lett*. **1996**, *69*, 1646.

(9) (a) Ulman, A. *Ultrathin Organic Film*; Academic Press: New York, 1991. (b) Ulman, A. *Chem. Rev*. **1996**, *96*, 1533.

(10) (a) Maoz, R.; Sagiv, J. *Langmuir* **1987**, *3*, 1034; (b) 1045.

(11) (a) Maoz, R.; Sagiv, J. *J. Colloid Interface Sci*. **1984**, *100*, 465. (b) Gun, J.; Sagiv, J. *J. Colloid Interface Sci.* **1986**, *112*, 457.

(12) Chen, S. H.; Frank, C. F. *Langmuir* **1989**, *5*, 978.

(13) (a) Schwartz, D. K.; Steinberg, S.; Israelachvili, J.; Zusadzinski, J. A. N. *Phys. Rev. Lett*. **1992**, *69*, 3354. (b) Xiao, X.-D.; Liu, G.; Charych, D. H.; Salmeron, M. *Langmuir* **1995**, *11*, 1600.

(14) (a) Bierbaum, K.; Grunze, M.; Baski, A. A.; Chi, L. F.; Schrepp, W.; Fuchs, H. *Langmuir* **1995**, *11*, 2143. (b) Banga, R.; Yarwood, J.; Morgan, A. M.; Evans, B.; Kells, J. *Langmuir* **1995**, *11*, 4393.

(15) Haran, A.; Waldeck, D. H.; Naaman, R.;. Moons, E.; Cahen, D. *Science* **1994**, *263*, 948.

(16) Wrighton, M. S.; Austin, R. G.; Bocarsly, A. B.; Bolts, J. M.; Haas O.; Legg, K. D.; Nadjo, L.; Palazzotto, M. C. *J. Am. Chem. Soc.* **1978**, *100*, 1602.

(17) Gu, Y.; Waldeck, D. H. *J. Phys. Chem. B* **1998**, *102*, 9015.

(18) Polymeropoulous, E. E.; Sagiv, J. *Chem. Phys.* **1978**, *69*, 1836.

(19) Sze, S. M. *Physics of Semiconductor Devices*, 2nd ed.; Wiley: New York, 1981.

(20) Levinshtein, M., Rumyantsev, S., Shur, M., Eds. *Handbook Series on Semiconductor Parameters*; World Scientific: New Jersey, **1996**; Vol. 1.

(21) Wasserman, S. R.; Tao, Y.; Whitesides, G. M. *Langmuir* **1989**, *5*, 1074.

(22) Sagiv, J. *Isr. J. Chem.* **1979**, *18*, 346.

(23) Shumaker, M. L.; Dollard, W. J.; Zeglinski, D. M.; Waldeck, D. H. *Proc. IS&T* **1991**, 231.

(24) Wagner, C. D.; Riggs, W. M.; Davis, L. E.; Moulder, J. F.; Muilenberg, G. E. *Handbook of X-ray Photoelectron Spectroscopy*; Perkin-Elmer: Eden Prairie, MN, 1979.

(25) Hochella, M. F., Jr.; Carim, A. H. *Surf. Sci. Lett*. **1988**, *197*, L260.

(26) (a) Pomykal, K. E.; Fajardo, A. M.; Lewis, N. S. *J. Phys. Chem.* **1995**, *99*, 8302. (b) Kumar, A.; Lewis, N. S. *J. Phys. Chem.* **1991**, *95*, 7021.

(27) Morrison, S. R. *Electrochemistry at Semiconductor and Oxidized Metal Electrodes*; Plenum: New York, 1980.

(28) The capacitance of the SAM overlayer will be in series with that of the oxide and the semiconductor depletion layer. Because of the high dopant density of the silicon, the measured capacitance is dominated by that of the oxide and the SAM. If one takes the dielectric constant of the SAM to be 2.6 and its thickness to be 2.5 nm, then one expects the serial capacitance to decrease by a factor of 0.285, which corresponds to an increase in $1/C^2$ of 12.2. The data in Figure 6 show an increase ranging from 11.6 to 13.6, in reasonable agreement with this simple analysis.

(29) (a) Wilson, R. H. *J. Appl. Phys*. **1977**, *48*, 4292. (b) Wilson, R. H. *CRC Crit. Rev. Solid State Mater. Sci.* **1980**, *10*, 1.

(30) (a) Haneman, D.; McCann, J. F. *Phys. Rev. B* **1982**, *25*, 1241. (b) McCann, J. F.; Haneman, D. *J. Electrochem. Soc*. **1982**, *129*, 1134 and references therein.

(31) Reiss, H. *J. Electrochem. Soc*. **1978**, *125*, 937.

(32) Gärtner, W. W. *Phys. Rev*. **1959**, *116*, 84.

(33) Reichman, J. *Appl. Phys. Lett*. **1980**, *36*, 574.

(34) The parameters used in modeling the current in the highly doped (10^{19} cm^{-3}) *n*-Si are given here. The hole mobility μ_p is 100 $cm^2/(V\ s)$. The absorption coefficient α is 3×10^3 cm^{-1}. The intrinsic carrier density n_i is 1.5×10^{10} cm^{-3}. The dielectric constant ϵ is 11.7. The flatband potential is -0.67 V versus SCE. The hole lifetime is taken to be 10 ns. The diode quality factor *m* is set to 1. The excess hole velocity at the space charge boundary with the bulk ($x = w$) was taken to be $\mu_p(2kTN_D/\pi\epsilon\epsilon_0)^{1/2}$. For the low dopant density (7.7×10^{15} cm^{-3}) simulations, the hole mobility was changed to 450 $cm^2/(V\ s)$ and the hole lifetime was 78 μs. The other parameters may be calculated from those given here or are reported in the text.

(35) Lewis, N. S. *J. Electrochem. Soc*. **1984**, *131*, 2496.

(36) Pierret, R. F. *Advanced Semiconductor Fundamentals*; Addison-Wesley: Reading, MA**,** 1987.

(37) (a) Kauffman, J. F.; Liu, C. S.; Karl, M. W. *J. Phys. Chem. B* **1998**, *102*, 2739. (b) Rosenwaks, Y.; Thacker, B. R.; Nozik, A. J.; Ellingson, R. J.; Burr, K. C.; Tang, C. L. *J. Phys. Chem.* **1994**, *98*, 2739.

(38) Adamson, A. W. *Physical Chemistry of Surfaces*, 5th ed.; Wiley: New York, 1990.